

## Ultrahigh damping in *R*-phase state of Ti–Ni–Fe alloy

Genlian Fan, Yumei Zhou, Kazuhiro Otsuka, and Xiaobing Ren<sup>a)</sup>

Multi-disciplinary Materials Research Center, Xi'an Jiaotong University, Xi'an 710049, China;

State Key Laboratory for Mechanical Behavior of Materials, Xi'an Jiaotong University, Xi'an 710049,

China; and Ferroic Physics Group, National Institute for Materials Science, Tsukuba 305-0047, Ibaraki, Japan

(Received 30 May 2006; accepted 31 August 2006; published online 16 October 2006)

Developing high damping materials with high strength is of significant technological importance, and Ti–Ni-based alloys are attracting much attention in this respect. The high damping peak in martensite state has been shown to be related to the interaction between twin boundary and hydrogen according to recent studies. In this letter the authors studied damping capacity of *R* phase in Ti<sub>50</sub>Ni<sub>48</sub>Fe<sub>2</sub> alloy, which has the lowest twinning shear among known martensites (*R*, *B19*, and *B19'*) in Ti–Ni-based alloys. They obtained a very high internal friction  $Q^{-1}=0.2$  for the relaxation-type peak in *R* phase, much higher than that for *B19* martensite or *B19'* martensite. Their results suggest that choosing martensite with smallest twinning shear (thus with the highest mobility) is an important guideline for developing very high damping materials. Furthermore, avoiding introducing precipitates and dislocations is also essential for obtaining high damping. © 2006 American Institute of Physics. [DOI: 10.1063/1.2363173]

Ti–Ni-based shape memory alloys have attracted much attention recently as high damping materials, since they exhibit both high internal friction (IF) and high strength.<sup>1,2</sup> In these martensitic alloys, two types of IF peaks may be observed. One is the transformation peak, which occurs at the martensitic transformation temperature range and is accompanied by a minimum in elastic modulus. This peak has strong dependence on cooling/heating rate, and the IF diminishes greatly if cooling/heating is stopped.<sup>3</sup> The other one is a relaxation-type peak occurring in the martensitic state, whose peak temperature shows a strong frequency dependence but does not correspond to a modulus minimum.<sup>4–11</sup> It is also called “broad peak,” because it extends over wide temperature range.<sup>4</sup> Since the peak is stable at constant temperature, the broad peak is much more important for practical applications compared with the transformation peak. Thus the critical issue in developing high damping materials is to increase the peak height and temperature range of the broad peak.

Much work has been done on the broad peak in *B19'* martensite of Ti–Ni (Refs. 5–7) and *B19* of Ti–Ni–Cu alloys.<sup>4,8–11</sup> Recent studies showed that hydrogen is essential for this peak.<sup>7–11</sup> By a critical experiment on Ti–Ni–Cu alloy with and without hydrogen, together with a study of nearly single domain sample, we have proven that the broad peak is due to the interaction between twin boundaries and hydrogen atoms.<sup>8</sup> In this letter we report an extraordinary high broad peak in *R* phase of Ti<sub>50</sub>Ni<sub>48</sub>Fe<sub>2</sub> alloy, much higher than the one in *B19'* martensite or *B19* martensite. We shall show that the ultrahigh damping peak in *R* phase is closely related to its small twinning shear.

Ti<sub>50</sub>Ni<sub>48</sub>Fe<sub>2</sub> samples sealed in quartz tubes with argon were annealed at 1173 K for 1 h and followed by water quenching. During such a process, the sample is naturally doped with hydrogen by a reaction between the absorbed H<sub>2</sub>O in the quartz tube and Ti in the samples during the high temperature solution treatment.<sup>8</sup> A small piece of Ti<sub>50</sub>Ni<sub>48</sub>Fe<sub>2</sub>

sample was tested by differential scanning calorimetry (DSC) to obtain the martensitic transformation temperature. Damping behavior of the sample was characterized by a dynamic mechanical analyzer (DMA). Samples with a size of 50×4.7×1.62 mm<sup>3</sup> were measured in dual cantilever constant-strain mode with an amplitude of 15 μm by a multifrequency isothermal method, i.e., we kept the sample at every measuring temperature for 5 min to reach thermal equilibrium and then changed the frequency from 0.2 to 20 Hz discretely. We call this “step cooling/heating” hereafter. More details about sample preparation and DMA measurement can be found in Ref. 8.

Figures 1(a) and 1(b) show the  $\tan \delta$  and storage modulus

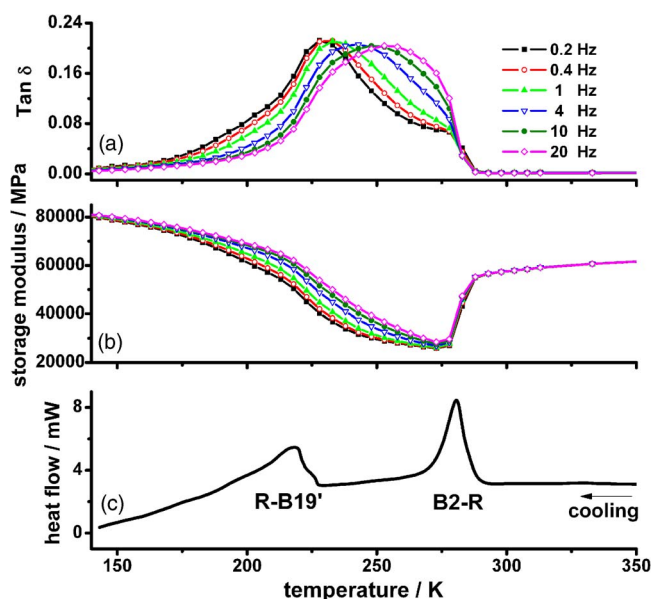


FIG. 1. (Color online) Internal friction  $\tan \delta$  (a) and storage modulus (b) as a function of temperature during step cooling for Ti<sub>50</sub>Ni<sub>48</sub>Fe<sub>2</sub> alloy by DMA. The sample was annealed at 1173 K for 1 h in a closed quartz tube filled with Ar and followed by water quenching. (c) DSC result on cooling for the sample with the same heat treatment.

<sup>a)</sup>Electronic mail: ren.xiaobing@nims.go.jp

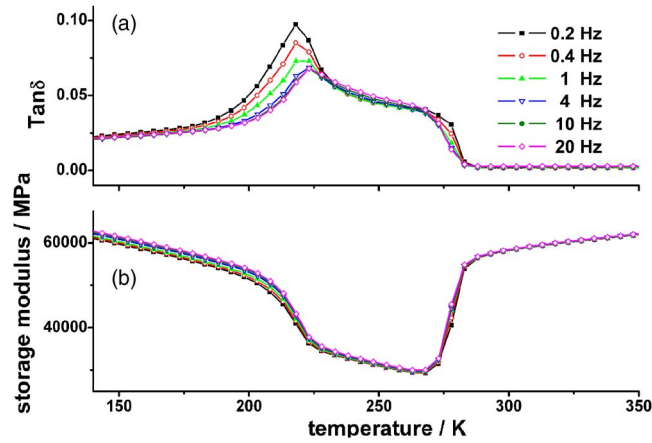


FIG. 2. (Color online) Internal friction  $\tan \delta$  (a) and storage modulus (b) as a function of temperature during step cooling for  $\text{Ti}_{50}\text{Ni}_{48}\text{Fe}_2$  alloy after dehydrogenation treatment at 1173 K for 1 h.

lus during step-cooling process. The  $B2$ - $R$  and  $R$ - $B19'$  transformation occur at 280 and 220 K, respectively, as identified by DSC measurement [Fig. 1(c)]. The  $B2$ - $R$  transformation manifests itself as a sudden increase of  $\tan \delta$  and a drastic decrease of modulus at about 280 K. This transformation peak is not as obvious as in ordinary cases because the transitory part was diminished due to the zero cooling rate.<sup>3,4</sup> The internal friction anomaly associated with the  $R$ - $B19'$  transformation at 220 K is not obvious, because there exists a huge damping peak in the  $R$ -phase regime (278–220 K) that smears such anomaly.

The most notable result of Fig. 1 is this ultrahigh damping peak of  $R$  phase, with a  $\tan \delta$  value ( $Q^{-1}$ ) as high as 0.2 (It is to be mentioned here that this extremely high  $Q^{-1}=0.2$  was already obtained in  $\text{Ti}_{50}\text{Ni}_{30}\text{Cu}_{20}$  alloy.<sup>4</sup> However, the value of IF depends on various factors such as the method of IF measurement, strain amplitude, frequency, etc. We will show later with respect to Fig. 3 that the IF associated with the broad peak in  $R$  phase is much higher than that in Ti–Ni–Cu by measuring IF under the same conditions.) This peak is our central interest in this letter. We notice that this peak and the associated storage modulus exhibit strong frequency dependence, and the peak temperature shifts to high temperature side with increasing frequency. The peak temperature and frequency show a good fit to Arrhenius relation, and activation energy and relaxation time are calculated to be  $E=0.73$  eV and  $\tau_0=1.2 \times 10^{-16}$  s. From the similarity of this  $R$ -phase peak with the broad peak for  $B19$  martensite in Ti–Ni–Cu,<sup>8</sup> it is natural to consider that they have the same origin, viz., the interaction of twin boundaries ( $R$  or  $B19$ ) with hydrogen, as proven in Ti–Ni–Cu system.<sup>8</sup> Supporting this view, Fig. 2 proves that the existence of H is a necessary condition for the existence of the high damping peak in  $R$  phase. This figure shows that the broad peak vanishes for a “dehydrogenated”  $\text{Ti}_{50}\text{Ni}_{48}\text{Fe}_2$  sample, i.e., hydrogen in the sample was eliminated by a vacuum treatment at 1173 K in a dynamic vacuum furnace (see Ref. 8 for details). Because of the disappearance of the broad peak, the transformation peak of  $R$ - $B19'$  martensitic transformation, which was smeared by the high damping peak in Fig. 1(a), can be clearly seen at about 220 K with a modulus minimum. The above analysis suggests that the broad peak in  $R$  phase has the same nature as that found in other martensites.

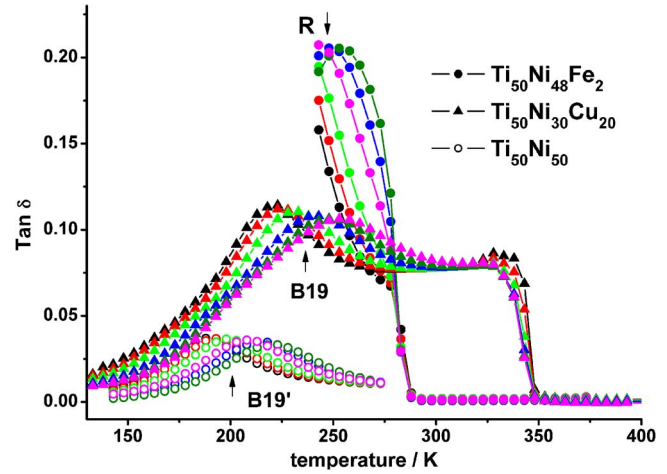


FIG. 3. (Color online) Comparison of the broad peak of  $R$  phase in  $\text{Ti}_{50}\text{Ni}_{48}\text{Fe}_2$  with that of  $B19$  in  $\text{Ti}_{50}\text{Ni}_{30}\text{Cu}_{20}$  and  $B19'$  in  $\text{Ti}_{50}\text{Ni}_{50}$  measured by DMA with amplitude of  $15 \mu\text{m}$ . Sample treatments and thickness:  $\text{Ti}_{50}\text{Ni}_{50}$ : 1273 K-1 h, 0.94 mm;  $\text{Ti}_{50}\text{Ni}_{30}\text{Cu}_{20}$ : 1273 K-1 h, 1.26 mm; and  $\text{Ti}_{50}\text{Ni}_{48}\text{Fe}_2$ : 1173 K-1 h, 1.62 mm.

Having known the nature of the ultrahigh damping peak for  $R$  phase, now we compare the height of  $R$ -broad peak in  $\text{Ti}_{50}\text{Ni}_{48}\text{Fe}_2$  with that of  $B19$  and  $B19'$  martensites in  $\text{Ti}_{50}\text{Ni}_{30}\text{Cu}_{20}$  and  $\text{Ti}_{50}\text{Ni}_{50}$ , respectively. Figure 3 shows the damping capacity of these martensites measured with the same amplitude of  $15 \mu\text{m}$ . The alloys were solution treated in the same way at 1173 or 1273 K for 1 h followed by water quenching. As can be seen in the figure, the  $R$ -broad peak in  $\text{Ti}_{50}\text{Ni}_{48}\text{Fe}_2$  alloy shows the highest value, about twice of that of  $B19$ -broad peak in  $\text{Ti}_{50}\text{Ni}_{30}\text{Cu}_{20}$  and six times higher than that of  $B19'$ -broad peak in  $\text{Ti}_{50}\text{Ni}_{50}$ . Why does the  $R$  phase exhibit much higher damping capacity than the other two martensites? We notice that these three martensites differ greatly in the size of twinning shear, as shown in Table I. Table I shows the major twinning system in these martensites,<sup>2,12–14</sup> where  $K_1$  represents twinning plane,  $\eta_1$  twinning shear direction, and  $s$  the amount of twinning shear. From this table we see that  $R$  phase has the extremely small twinning shear;  $B19$  martensite does next, and  $B19'$  has the largest twinning shear. The size of twinning shear determines the ease of twinning process and thus the mobility of the twin boundaries. This determines to a large extent the magnitude of damping capacity, because the damping peak discussed here is associated with twin boundary motion. The relation between the magnitude of damping capacity and twinning shear, as discussed above, seems to suggest an im-

TABLE I. Comparison of twinning shear in three martensite structures.

Structure of martensite	$K_1$	$\eta_1$	$s$	Ref.
$B19'$ (monoclinic)	$\{0.720, 1, \bar{1}\}$	$\langle 011 \rangle$	0.280	2
	$\{\bar{1}\bar{1}1\}$	$\langle 0.540, 0.459, 1 \rangle$	0.310	
$B19$ (orthorhombic)	$\{111\}$	$\langle 5.88, \bar{1}, 4.88 \rangle$	0.170	12
	$\{011\}$	$\langle 01\bar{1} \rangle$	0.110	
$R$ (in hexagonal index)	$\{11\bar{2}1\}$	$\langle 11\bar{2} \rangle$	0.0265 <sup>a</sup>	13
	$\{11\bar{2}\bar{2}\}$	$\langle 111 \rangle$	0.0265 <sup>a</sup>	14

<sup>a</sup>The value of  $s$  was taken from Ref. 14, since  $s$  is a function of temperature. This corresponds to  $\alpha=89.46^\circ$  at  $T=(T_R-35)$  K for  $R$  phase.

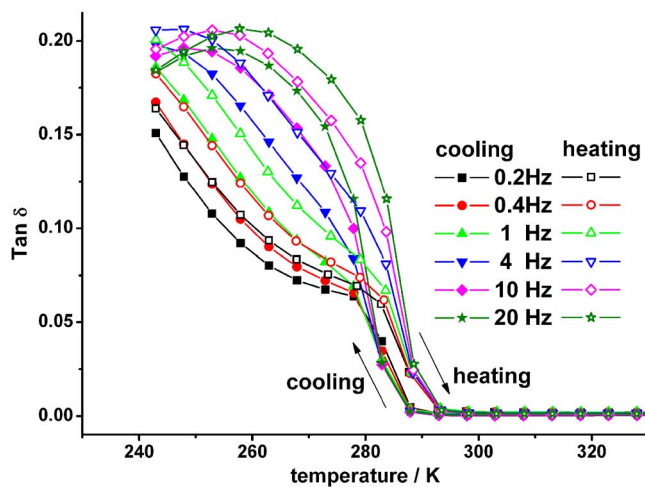


FIG. 4. (Color online) Partial DMA cycling between *R* phase and *B2* phase upon step cooling (closed symbols) and step heating (open symbols).

portant guideline for developing high damping materials: high damping can be obtained by using the martensitic structure with the smallest twinning shear. The *R* phase is superior to other martensites in this respect. Besides the ultrahigh damping capacity, Ti–Ni–Fe alloy has high ductility and strength. This provides a possibility to develop high damping materials with good mechanical properties.

Although *R* phase has very high damping capacity associated with the interaction of twin boundary and hydrogen, the damping capacity may be significantly lowered if the twin boundaries are anchored by obstacles such as precipitates or dislocations. It has been found that *R*-phase alloy containing many small precipitates (aged Ti–51Ni alloy) exhibits a much lower internal friction peak ( $Q^{-1}=0.04$ ).<sup>15</sup> In Ti–Ni binary alloy, dislocations can be generated simply by transformation cycling due to the large transformation strain,<sup>1,2</sup> thus the broad peak is expected to lower with transformation cycling. It was indeed found to be true.<sup>5</sup> In the present case, the small transformation strain of *B2*–*R* transformation (about 1%) guarantees the stability of *R*-broad peak because no dislocation will be introduced to the alloy during transformation cycling between *B2* and *R* phases. Figure 4 shows the result of the sample subjected to one DMA thermal cycling between *B2* and *R* phases. We can see that the peak height keeps its original value after one thermal cycle, which is very important for application. Considering

the above, we may come to a second guideline for obtaining high damping: avoiding introducing obstacles such as dislocations and precipitates is essential for high damping. Nevertheless, we have to admit that the only shortcoming of *R*-broad peak in Ti<sub>50</sub>Ni<sub>48</sub>Fe<sub>2</sub> alloy is that the transformation temperature of *B2*–*R* is not high enough. If we can increase the *B2*–*R* transformation temperature to above room temperature, the high *R*-broad peak may be used at room temperature. Further work should be done in this direction.

To summarize, it was shown that extremely high and stable internal friction peak of relaxation type is available by utilizing the interaction between highly mobile *R* phase twin boundaries and hydrogen in Ti<sub>50</sub>Ni<sub>48</sub>Fe<sub>2</sub> alloy. This will be very useful for practical applications, since the present alloy not only exhibits high damping but also possesses high strength and high ductility.

The authors acknowledge the support of Kakenhi of JSPS and a special fund for Cheungkong professorship, National Science Foundation of China, 111 project of China, as well as National Basic Research Program of China under Grant No. 2004CB619303. The authors thank T. Suzuki, J. Sun, K. Nakamura, F. Yin, I. Yoshida, L. Zhang, Y. Wang, D. Ding, J. Zhang, and W. Chen for helpful discussions.

<sup>1</sup>Shape Memory Materials, edited by K. Otsuka and C. M. Wayman (Cambridge University Press, Cambridge, 1998), Chaps. 3 and 7.

<sup>2</sup>K. Otsuka and X. Ren, Prog. Mater. Sci. **50**, 511 (2005).

<sup>3</sup>J. San Juan and M. L. N  , J. Alloys Compd. **355**, 65 (2003).

<sup>4</sup>I. Yoshida, D. Monma, K. Iino, K. Otsuka, M. Asai, and H. Tszuzuki, J. Alloys Compd. **355**, 79 (2003).

<sup>5</sup>J. S. Zhu, R. Schaller, and W. Benoit, Phys. Lett. A **141**, 177 (1989).

<sup>6</sup>H. C. Lin, S. K. Wu, and Y. C. Chang, Metall. Mater. Trans. A **26A**, 851 (1995).

<sup>7</sup>F. M. Mazzolai, B. Coluzzi, G. Mazzolai, and A. Biscarini, Appl. Phys. Lett. **85**, 2756 (2004).

<sup>8</sup>G. Fan, Y. Zhou, K. Otsuka, X. Ren, K. Nakamura, T. Ohba, T. Suzuki, I. Yoshida, and F. Yin, Acta Mater. (in press).

<sup>9</sup>T. Sakaguchi, T. Uehara, Y. Kogo, S. Takeuchi, and N. Igata, Mater. Trans. **46**, 1306 (2005).

<sup>10</sup>F. M. Mazzolai, A. Biscarini, R. Campanella, B. Coluzzi, G. Mazzolai, A. Rotini, and A. Tuissi, Acta Mater. **51**, 573 (2003).

<sup>11</sup>A. Biscarini, B. Coluzzi, G. Mazzolai, F. M. Mazzolai, and A. Tuissi, J. Alloys Compd. **356–357**, 669 (2003).

<sup>12</sup>Y. Watanabe, T. Saburi, Y. Nakagawa, and S. Neuno, J. Jpn. Inst. Met. **54**, 861 (1990) [in Japanese].

<sup>13</sup>T. Fukuda, T. Saburi, K. Doi, and S. Nenno, Mater. Trans., JIM **33**, 271 (1992).

<sup>14</sup>S. Miyazaki and C. M. Wayman, Acta Metall. **36**, 181 (1988).

<sup>15</sup>H. C. Lin, S. K. Wu, and T. S. Chou, J. Alloys Compd. **355**, 90 (2003).